Effects of Shockley-Read-Hall recombination on the reflection sensitivity of quantum dot lasers directly grown on silicon

Zhao, S., Duan, J., Dong, B., Grillot, F.

Effects of Shockley-Read-Hall recombination on the reflection sensitivity of quantum dot lasers directly grown on silicon

S. Zhao[a,*], J. Duan[b], B. Dong[a], and F. Grillot[a,c]

[a]LTCI, Institut Polytechnique de Paris, Télécom Paris, 19 place Marguerite Perey, 91120, Palaiseau, France
[b]State Key Laboratory on Tunable Laser Technology, School of Electronic and Information Engineering, Harbin Institute of Technology, Shenzhen, 518055, China
[c]Center for High Technology Materials, University of New-Mexico, Albuquerque, NM, USA

ABSTRACT

Photonics integrated circuits on silicon are considered as a key technology for data centers and high-performance computers. Owing to the ultimate carrier confinement and reduced sensitivity to crystalline defects, semiconductor quantum dot lasers directly grown on silicon exhibit remarkable properties such as low threshold current, high temperature stability and robust tolerance to external reflections. This latter property is particularly important for achieving large-scale integrated circuits whereby unintentional back-reflections produced by the various passive/active optoelectronic components can hinder the stability of the lasers. In this context, it is known that quantum dot lasers are more resistant to optical feedback than quantum well ones thanks to the low linewidth enhancement factor, the large damping, and the possible absence of upper lasing states. In this work, we theoretically investigate the reflection sensitivity of quantum dot lasers directly grown on silicon by studying the peculiar role of the epitaxial defects, which induce nonradiative recombination through the Shockley-Read-Hall process. By using the Lang and Kobayashi model, we analyze the nonlinear properties of such quantum dot lasers through the bifurcation diagrams and with respect to the nonradiative lifetime. In particular, we show that the increase of the Shockley-Read-Hall recombination shrinks the chaotic region and shifts the first Hopf bifurcation to higher feedback values. We believe that these results can be useful for designing novel feedback resistant lasers for future photonics integrated circuits operating without optical isolator.

Keywords: quantum dots laser, silicon photonics, laser dynamics, bifurcation diagram

1. INTRODUCTION

A unique feature of semiconductor lasers is their low tolerance for external optical feedback (EOF). The physical processes involved in a semiconductor laser under EOF rely on the so-called phase-amplitude coupling driven by the linewidth enhancement factor (α-factor) in the active region between the returned light field and the intracavity field.[1] Optical feedback is coupled into the laser cavity through the output facet and causes a perturbation on the photon density hence leading to a fluctuation of the carrier density and thus the optical gain. The intensity fluctuation is then modulated by the damping effect and linked to the optical gain, where the gain variation itself impacts on the refractive index through the α-factor which produces a shift in the lasing wavelength. In a high-speed communication system, EOF must be absolutely avoided because severe temporal instabilities in the laser's output (eg. coherence collapse) can affect the quality of the data transmission.[2] In order to counter these unwanted back-reflections, the inclusion of expensive and bulky optical isolators are required in order to maintain the laser's stability. Consequently, the development of feedback insensitive transmitters remains of paramount importance especially for silicon-based integrated technologies where current on-chip optical isolators do not exhibit yet sufficient isolation ratio and insertion loss.[3]

Owing to their quasi-class A behavior, quantum dot (QD) lasers display a natural higher dynamical stability against EOF than conventional bulk and quantum well (QW) ones. As they exhibit less complicated trajectories and smaller region of chaotic dynamics, QD lasers offer a great potential for reflection insensitivity. The improved

---

*shiyuan.zhao@telecom-paris.fr

performance of QD lasers against EOF is linked to their large damping factor and reduced phase-amplitude coupling.[4] It was also proved that QD lasers emitting on the sole ground state (GS) transition are more stable than those operating on the excited state (ES) or within the dual-state lasing regime (GS + ES).[5] In addition, the higher threading dislocations (TD) and epitaxial defects induced shorter carrier lifetime is also touted to further enhance the stability of the laser against EOF. Indeed, the epitaxial growth causes a high density of defects which induces non-radiative recombination through the Shockley-Read-Hall (SRH) process.[6] All these features make QD lasers excellent candidates for isolation-free related applications.[7] The motivation of this work is to better analyze the influence of the nonradiative recombination on the QD laser's optical feedback sensitivity. To do so, we investigate both numerically and analytically the case of an epitaxial QD laser on silicon subjected to EOF. With the increase of the SRH recombination, the first Hopf bifurcation is found to occur at higher feedback levels whereas the chaotic bubbles is smoothly eliminated. The results are found in agreement with the recent experiments hence confirming the enhanced stability of such epitaxial QD lasers against EOF. Overall, this work brings further insights in the understanding of QD laser physics, which are useful for designing feedback resistant lasers for isolation-free applications in photonics integrated circuits.

2. NUMERICAL MODEL

The QD model is established to take into account the EOF produced by a distant reflector of amplitude reflectivity r_3. We use the Lang and Kobayashi (LK) approach which is based on two ordinary delay differential equations for the complex electrical field and for the carrier number.[8] The LK model is well-suitable for analyzing the nonlinear dynamics of a semiconductor laser under EOF hence highlighting many complex behaviors like mode hopping, low-frequency fluctuations (LFF), the onset of the coherence collapse, and coexisting attractors with time-periodic intensities. In what follows, it has to be noted that multiple round-trips of the electric field in the external cavity are excluded, as the effective feedback strength for such round-trips rapidly decreases, which restricts the validity of the model to low feedback levels.[9] Also, the Langevin noises should be taken into account to fully understand the transient and dynamical behaviors of the semiconductor laser. In this work, the Langevin noises are not considered in order to separate the deterministic chaos from the stochastic noise. As a consequence of that, the QD laser's differential equations read as follows:

$$\frac{dN}{dt} = J - \frac{N}{\tau_c} - G_N(N(t) - N_0)|E|^2 \tag{1}$$

$$\frac{dE}{dt} = \frac{1 + i\alpha}{2}(G_N(N(t) - N_0) - \frac{1}{\tau_p})E + \frac{k}{\tau_{in}}E(t - \tau)e^{-i\omega_0\tau} \tag{2}$$

with τ_p, τ_{in}, τ and τ_c the photon lifetime, the cavity round-trip time, the external cavity round-trip time, and the carrier lifetime, respectively. Other parameters are k the power reflected from the external cavity with respect to that from the laser mirror and J the pumping term. The solitary laser is assumed to oscillate in a single longitudinal mode with angular frequency ω_0 while N_0 is the carrier density at the transparency for the solitary laser and G_N the dynamic gain defined as $G_N = \partial G/\partial N$. Using a dimensionless form, the LK equations describing the complex electrical field Y and the carrier number Z are given by:[10]

$$\frac{dY}{ds} = (1 + i\alpha)ZY + \eta e^{-i\Omega\theta}Y(s - \theta) \tag{3}$$

$$T\frac{dZ}{ds} = P - Z - (1 + 2Z)|Y|^2 \tag{4}$$

with $s = t/\tau_p$ and Ω the dimensionless angular frequency of the solitary laser. We note $T = \tau_c/\tau_p$ as the ratio of the carrier lifetime to photon lifetime, $\theta = \tau/\tau_p$ the ratio of the external cavity round-trip time to the photon lifetime, P the dimensionless pumping current above threshold, and $\eta > 0$ the feedback strength. In what follows r_3 is treated as the bifurcation parameter proportional to η. As aforementioned stated, the epitaxial growth of InAs QDs on silicon substrate embrace several challenges such as the control of the epitaxial defects which introduce nonradiative recombination centers through the SRH process.[11] The relation between the nonradiative recombination lifetime and the defect density can be written as follows:[12]

$$\frac{1}{\tau_{SRH}} = \frac{1}{\tau_{SRH}^0} + \frac{D\pi^3\sigma}{4} \tag{5}$$

with τ_{SRH}^0 the lifetime of dislocation-free GaAs-based QD lasers, D the diffusion coefficient and σ the TD density. The defect density in GaAs-based QD lasers is typically in a range of 10^3–10^4cm^{-2} or less, and the corresponding τ_{SRH} is on the order of 10 ns, which is much longer than the spontaneous emission lifetime ($\sim$1.0 ns). Therefore, in QD lasers grown on native substrate, this additional nonradiative recombination term can be neglected in the simulations.[13] However, a different situation occurs in silicon-based QD lasers where the defect density (10^6–10^8cm^{-2}) is at least two orders of magnitude higher than that in GaAs-based QD ones.[14] Here, the nonradiative carrier lifetime can be as low as 0.1 ns, therefore becoming shorter than the spontaneous emission lifetime. To account for this phenomenon, the carrier equation (eq.(1)) is reformulated as follows:

$$\frac{dN}{dt} = J - \frac{N}{\tau_c} - \frac{N}{\tau_{SRH}} - G_N(N(t) - N_0)|E|^2 \tag{6}$$

where the effective carrier lifetime (τ_c') is indeed shortened by the SRH process through the relationship:

$$\frac{1}{\tau_c'} = \frac{1}{\tau_c} + \frac{1}{\tau_{SRH}} \tag{7}$$

3. NUMERICAL RESULTS

The effect of the nonradiative recombination on the QD laser's feedback sensitivity is analyzed through the bifurcation diagram. The evolution of the first Hopf bifurcation along with the chaotic bubbles are analyzed and discussed. Equations (1)–(2) can be solved numerically by using the fourth-order Runge–Kutta method. The simulation parameters for the QD laser are given in Table 1 if not otherwise specified. In the simulations, the time step is 0.5 ps and the time span is 2 μs.

In this section, we compare the bifurcation diagrams obtained by considering different values of the SRH lifetime

Table 1. Material and optical parameters of the QD laser during the simulation

Symbol	Description	Value
G_N	Gain coefficient	8.4×10^{-13}m^{3}s^{-1}
N_0	Carrier density at transparency	1.4×10^{24}m^{-3}
τ_p	Photon lifetime	1.927×10^{-12}s
τ_c	Carrier lifetime	2×10^{-9}s
τ_{in}	Round-trip time in internal cavity	8.0×10^{-12}s
τ_{SRH}	nonradiative recombination lifetime	0.1$\sim$10 ns (*variable*)
r_2	Reflectivity of laser facet	0.5
r_3	Reflectivity of external mirror	0.01 (*variable*)
$j = J/J_{th}$	Normalized injection current	1.01
L	External cavity length	0.3 m
α	Linewidth enhancement factor	2
λ	Optical wavelength	1.5×10^{-6}m
c	Speed of light	2.9×10^8ms^{-1}
$\tau = 2L/c$	Round-trip time of feedback light in external cavity	2.0×10^{-9}s
$\omega = 2\pi c/\lambda$	Optical angular frequency	1.2×10^{15}s^{-1}

according to the equation (5) which was derived from an approximation method.[12] Fig.1 shows the evolution of the SRH lifetime with respect to the TD density, assuming the latter varying from 10^5 cm^{-2} to 10^7 cm^{-2}. The non radiative recombination process is found inversely proportional to the TD density. The simulation shows that the SRH lifetime ranges from 0.1 ns to 7 ns, which validates the parameters taken in Table.1. In order to
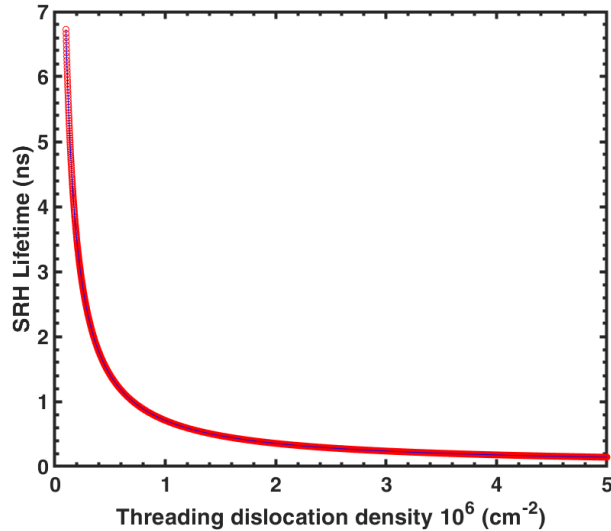
Figure 1. SRH lifetime obtained by an approximation method as a function of threading dislocation density.

further investigate the influence of the SRH lifetime on the chaotic dynamics and the first Hopf bifurcation, we start by analyzing the situation of an epitaxial QD laser operating right above the threshold $(1.01 \times J_{th})$ with $\alpha=2$. Even if it was shown that the α factor of an epitaxial QD laser can be as low as 0.32,[15] we consider here a larger value to better emphasize the impact of this parameter on the bifurcation diagram. Fig.2 displays the computed bifurcation diagram that is to say the evolution of the local extremums of the normalized intensity as a function of the bifurcation parameter r_3 and for different values of the SRH lifetime. In the simulations, the external cavity length is fixed to 30 cm. Fig.2(a) shows that when r_3 is increased from zero, the first external cavity mode (ECM) is initially stable and then undergoes a Hopf bifurcation, indicating the birth of sustained relaxation oscillations. The laser becomes unstable and enter a chaotic bubble via a period-doubling bifurcation. For $r_3 = 0.0044$, the next higher ECM (mode 2) becomes stable and temporarily coexists with the unstable mode 1. For these values of r_3, the second ECM (mode 2) is stable and corresponds to the maximum gain mode.[16] Then, mode 2 undergoes a Hopf bifurcation for $r_3 = 0.0171$ and follows a dynamic route from quasi-periodic to chaos as shown for $r_3 = 0.0265$. For a further increase of r_3, the next ECM (mode 3) is initially stable, then undergoes a Hopf bifurcation following a similar route into instabilities, and the bifurcation cascade continues.[17] The computed time series corresponding to the different vertical blue dash-dotted lines represented in Fig.1(a) are displayed in Fig.3. It shows that from (a) to (d), the increase of r_3 leads to chaotic oscillations through period-doubling.

The impact of the SRH lifetime on the bifurcation diagram is also unlocked in Fig.2. Any decrease of τ_{SRH} from (a) to (d) makes the bifurcation diagram of less complexity. As we can see, the different chaotic bubbles are smoothly eliminated when reducing the nonradiative lifetime, eventually at $\tau_{SRH} = 0.1$ ns, the chaotic window disappears leaving only small periodic oscillations. Nevertheless, at a large feedback strength ($r_3 = 0.0384$), the blue square window in Fig.2(d) reveals the emergence of LFFs, which is a peculiar signature of low-dimensional deterministic chaos.[18] The time series in Fig.4 confirms the LFF characteristics where the laser intensity starts to exhibit sudden dropouts at irregular time intervals, followed by a gradual recovery. And the time scale of these fluctuations is long compared to the intrinsic time scale of the laser oscillations. Last but not least, it is important to stress that the first Hopf bifurcation is found to be dependent on τ_{SRH}. Thus, as we can see in Fig.4(b), when τ_{SRH} decreases, the first Hopf bifurcation occurs at larger values of r_3, which means that the stable operation area associated with mode 1 is expanded. In recent experiments, the epitaxial QD laser on silicon demonstrated a remarkable stability against EOF without showing any chaotic operation. This intrinsic feature was explained thanks to the large damping, the low α, and the absence of higher energy states in the lasing emission process. Here, we think that the SRH recombination are additional mechanisms that play a role in the evolution of the reflection sensitivity. Shortening τ_{SRH} increases the resistance against EOF which is exactly what happens in epitaxial QD lasers as compared to their counterparts grown on native substrate.
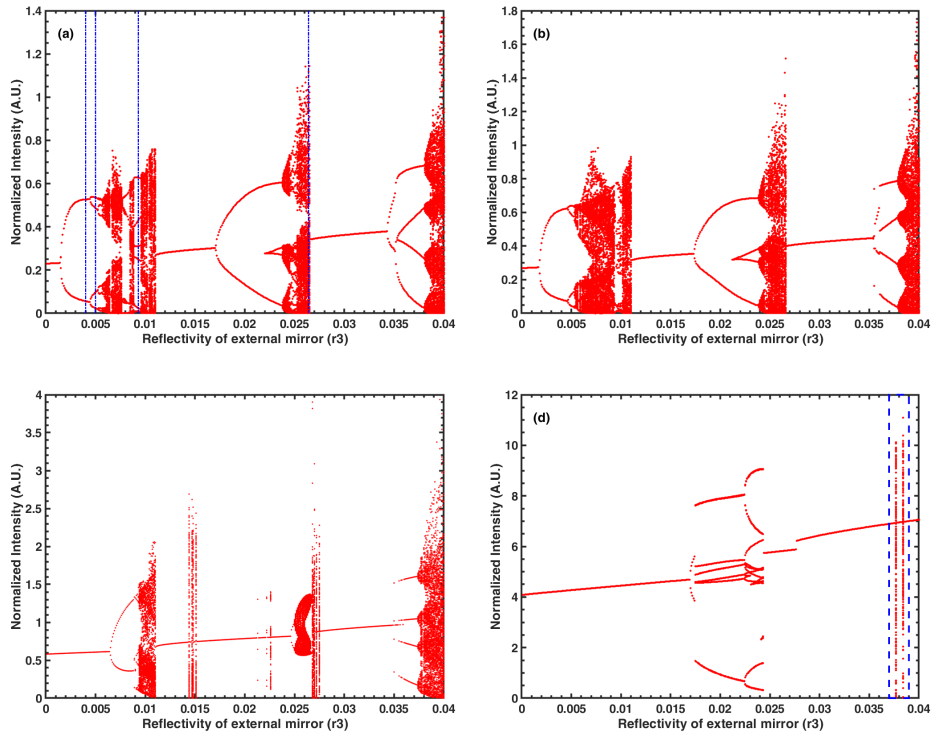
Figure 2. Computed bifurcation diagrams of local extremums of the normalized intensity as a function of the bifurcation parameter r_3 for $\alpha=2$ and different values of τ_{SRH}: (a) τ_{SRH}=10 ns; (b) τ_{SRH}=5 ns; (c) τ_{SRH}=1 ns; (d) τ_{SRH}=0.1 ns.
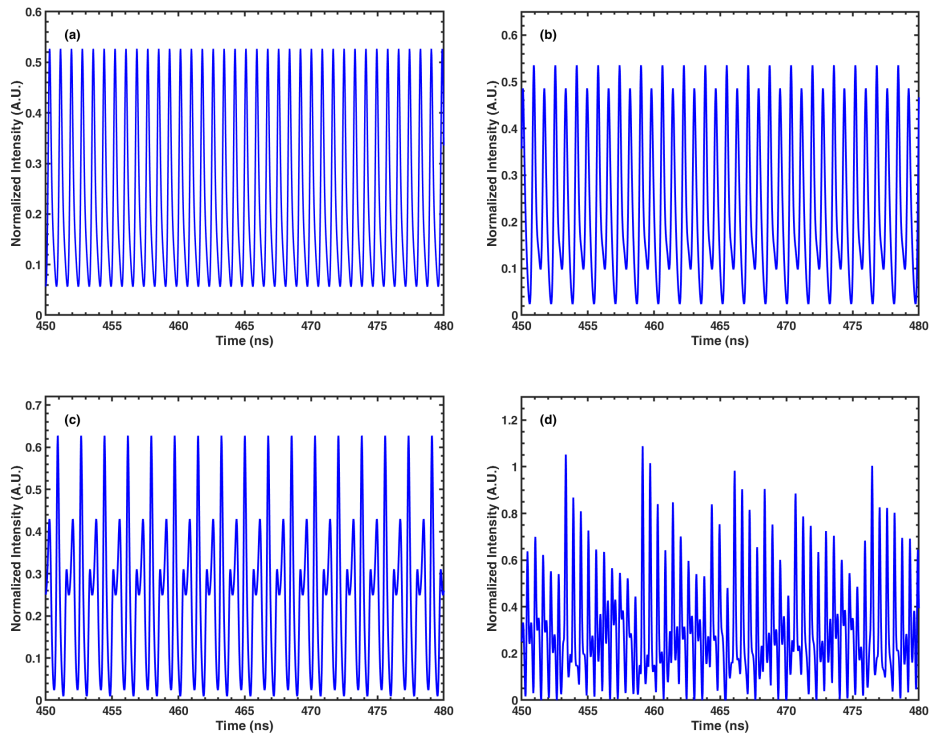

Figure 3. Computed time series for different values of r_3 and τ_{SRH}. From left to right, $r_3 = 0.004$, 0.005, 0.0093, 0.0264 respectively, which correspond to the vertical blue dash-dotted lines displayed in Fig.1(a).
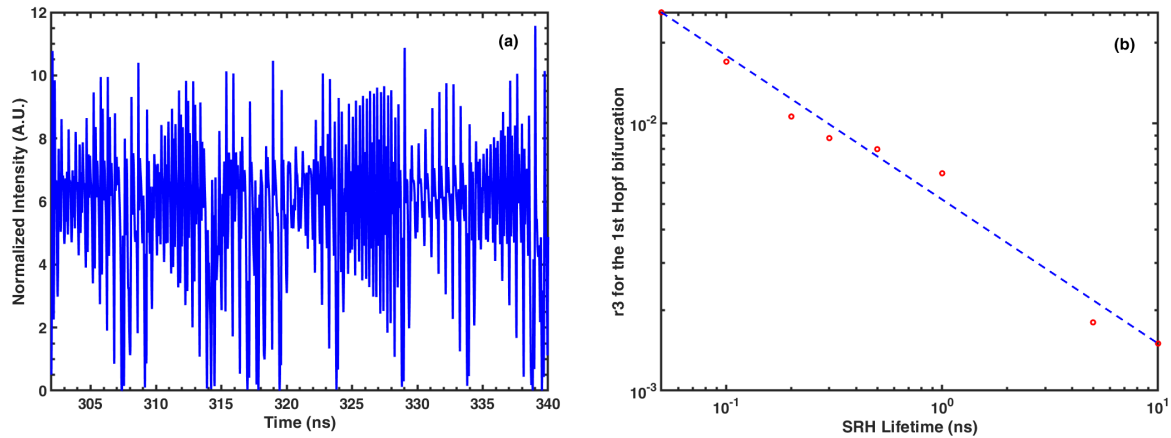
Figure 4. (a) Computed time series for τ_{SRH}=0.1 ns corresponding to the blue dash-dotted rectangle displayed in Fig.1(d); (b) The evolution of the first Hopf bifurcation with respect to the different values of SRH recombination lifetime according to the Fig.2. The dashed line is used for guiding the eyes only.

Let us now focus on a real configuration assuming an external cavity length of 4 cm which simulates the situation of a very short reflection as that occurring on a PIC. The QD laser is still pumped right above the threshold ($1.01 \times J_{th}$) but now the α is taken at 0.5 to fully match the experimental value.[4] Simulations depicted in Fig.5 are obtained for two values of τ_{SRH}. It is clear that the bifurcation diagrams do not show a signature with a wide chaotic dynamics. As we can see for τ_{SRH}=10 ns, there only exists the stable solution taking place after a region located at low feedback levels where periodic oscillations coexist with a narrow chaotic region. Ultimately when τ_{SRH}=0.1 ns, the chaotic region vanishes leaving the periodic oscillation. The results are consistent with the above-threshold simulations obtained with a larger α. In addition, we also confirm that lowering τ_{SRH} slightly moves the first Hopf bifurcation point to the higher values of r_3 here from r_3=0.02 to r_3=0.03.
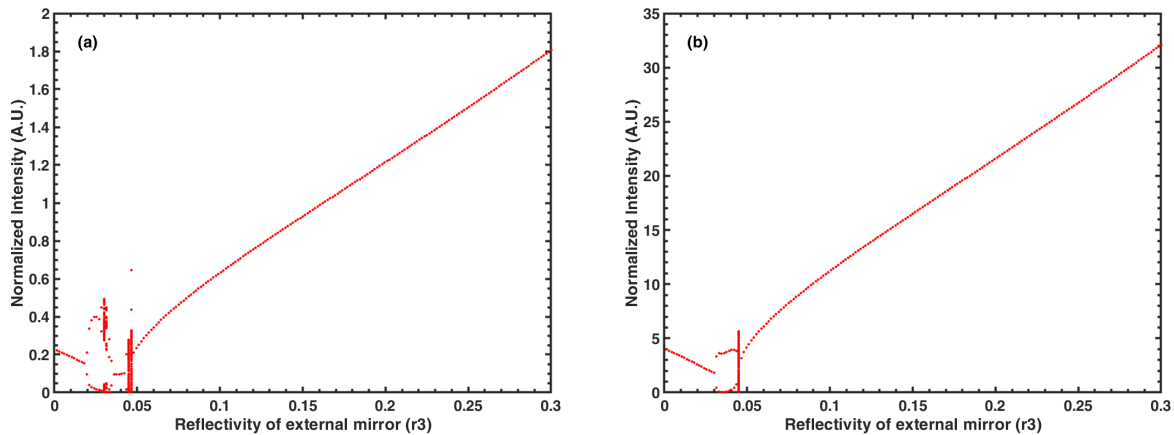

Figure 5. Computed bifurcation diagrams for an cavity length of 4 cm. (a) left, α=0.5 and τ_{SRH}=10 ns; (b) Right, $\alpha = 0.5$ and τ_{SRH}=0.1 ns

4. ANALYTICAL METHOD

Analyzing the steady state solutions and their linear stability properties lead to valuable information on the effects of some parameters and, possibly, scaling arguments which may be used to simplify the nonlinear problem. In this section, we put in practice these ideas by investigating the Hopf bifurcation that is to say the bifurcation from a steady state intensity to limit-cycle intensity oscillations. A Hopf bifurcation often marks the first instability

of a cascade of successive bifurcations to gradually more complex responses.[17] A basic solution of Eqs.(3) and (4) is a single frequency solution of the form:

$$Y = A_s e^{i(\Omega_s - \Omega_0)s}$$
$$Z = Z_s$$

where A_s, Ω_s and Z_s are constants. Substituting these equations into Eqs.(3) and (4) leads to three equations for these constants while $\Delta = \Omega_s \theta$ the external cavity mode frequency satisfies the following transcendental equation:

$$\Delta - \Omega_0 \theta = -\eta\theta(\alpha \cos\Delta + \sin\Delta)$$

The intensity of the laser field is then given by

$$A_s^2 = \frac{P + \eta\cos\Delta}{1 - 2\eta\cos\Delta} \geq 0$$

where the inequality restricts the possible values of Δ. As η progressively increases from zero, the number of possible ECM increases too. Let us determine the conditions for a Hopf bifurcation from a single frequency solution. From the linearized equations, we determine the characteristic equation for the growth rate λ. The condition for a Hopf bifurcation is obtained by substituting $\lambda = i\omega$ into the characteristic equation. Then by separating the real and imaginary parts, one obtain two equations for the feedback rate η and the frequency ω of the oscillations at the Hopf bifurcation point.[19] These equations are transcendental which means that they are difficult to solve numerically. However, approximations were proposed assuming that $\epsilon = 1/T$ is $\mathcal{O}(10^{-3})$ a small quantity.[20] Seeking a solution in power series of $\epsilon^{1/2}$ leads to the following relationships for η and ω

$$\eta = -\epsilon\frac{1 + 2P}{2\sin^2(\frac{\omega\theta}{2})(\cos\Delta + \alpha\sin\Delta)} \tag{8}$$

$$\omega = \omega_R + \epsilon\frac{1 + 2P}{2}\cot\omega\theta \tag{9}$$

where $\omega_R = (2P\epsilon)^{1/2}$ is the relaxation oscillation frequency of the laser. Because $\eta\theta$ is $\mathcal{O}(\epsilon^{1/2})$, we find that $\Delta \simeq \Omega_0\theta$. The approximation of ω is valid for all values of P except at and near points of resonance verifying the condition $\omega_R = 2n\pi\theta^{-1}(n=0,1,2,3...)$. At these values of ω_R, the denominator in Eqs.(8) is zero. Inner solutions can be constructed near these points but become inadequate if θ is increased. Fig.6 displays the evolution of η corresponding to the first Hopf bifurcation as a function of τ_{SRH}. The blue curve is obtained from Eq.(8) whereas the red one corresponds to the extraction of the valid data. It is straightforward that when SRH lifetime decreases, the feedback strength η increases, which means that the first Hopf bifurcation is shifted to stronger optical feedback. Such a result agrees with the numerical simulations depicted in the previous section.

5. CONCLUSION

In summary, we have investigated numerically the impact of the SRH lifetime on the feedback stability of a QD laser directly grown on silicon. By considering different τ_{SRH} values, we show that the chaotic region shrinks and that the first Hopf bifurcation is shifted to higher feedback values. In addition, an analytical method based on the asymptotic approximation was found to nicely reproduce the same tendency. Such results indicate that epitaxial QD lasers do have a strong robustness against EOF which is of paramount importance for the next generation of cost-effective PICS operating without optical isolators.

REFERENCES

[1] Kane, D. M. and Shore, K. A., [*Unlocking dynamical diversity: optical feedback effects on semiconductor lasers*], John Wiley & Sons (2005).

[2] Grillot, F., Norman, J. C., Duan, J., Zhang, Z., Dong, B., Huang, H., Chow, W. W., and Bowers, J. E., "Physics and applications of quantum dot lasers for silicon photonics," *Nanophotonics* **1**(ahead-of-print) (2020).
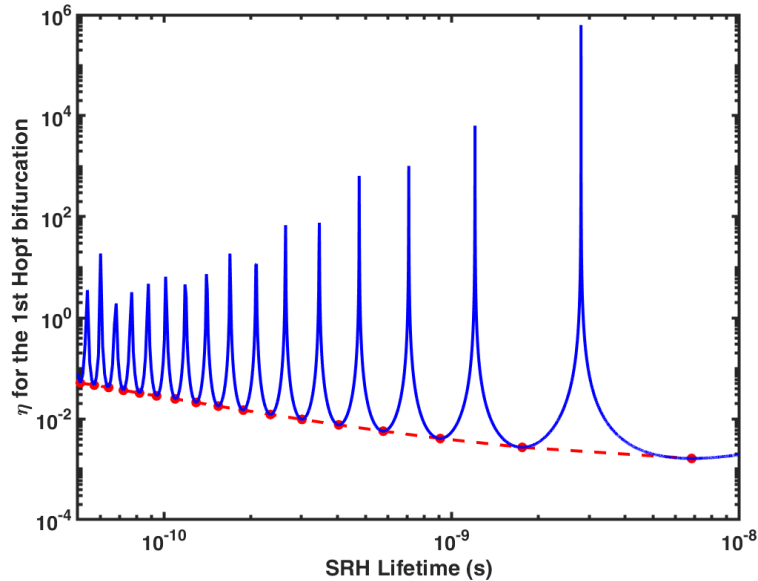
Figure 6. The asymptotic method for the first Hopf bifurcation point. The blue curve is obtained from Eq.8 whereas the red one is the good extraction of the valid data.

[3] Zhang, Y., Du, Q., Wang, C., Fakhrul, T., Liu, S., Deng, L., Huang, D., Pintus, P., Bowers, J., Ross, C. A., et al., "Monolithic integration of broadband optical isolators for polarization-diverse silicon photonics," *Optica* **6**(4), 473–478 (2019).

[4] Duan, J., Huang, H., Jung, D., Zhang, Z., Norman, J., Bowers, J., and Grillot, F., "Semiconductor quantum dot lasers epitaxially grown on silicon with low linewidth enhancement factor," *Applied Physics Letters* **112**(25), 251111 (2018).

[5] Huang, H., Lin, L.-C., Chen, C.-Y., Arsenijević, D., Bimberg, D., Lin, F.-Y., and Grillot, F., "Multimode optical feedback dynamics in InAs/GaAs quantum dot lasers emitting exclusively on ground or excited states: transition from short-to long-delay regimes," *Optics Express* **26**(2), 1743–1751 (2018).

[6] Zhou, Y.-G., Zhao, X.-Y., Cao, C.-F., Gong, Q., and Wang, C., "High optical feedback tolerance of InAs/GaAs quantum dot lasers on germanium," *Optics Express* **26**(21), 28131–28139 (2018).

[7] Duan, J., Huang, H., Dong, B., Jung, D., Norman, J. C., Bowers, J. E., and Grillot, F., "1.3-μm reflection insensitive InAs/GaAs quantum dot lasers directly grown on silicon," *IEEE Photonics Technology Letters* **31**(5), 345–348 (2019).

[8] Lang, R. and Kobayashi, K., "External optical feedback effects on semiconductor injection laser properties," *IEEE Journal of Quantum Electronics* **16**(3), 347–355 (1980).

[9] Van Tartwijk, G. and Lenstra, D., "Semiconductor lasers with optical injection and feedback," *Quantum and Semiclassical Optics: Journal of the European Optical Society Part B* **7**(2), 87 (1995).

[10] Alsing, P., Kovanis, V., Gavrielides, A., and Erneux, T., "Lang and kobayashi phase equation," *Physical Review A* **53**(6), 4429 (1996).

[11] Norman, J., *Quantum Dot Lasers for Silicon Photonics*, PhD thesis, UC Santa Barbara (2018).

[12] Saldutti, M., Tibaldi, A., Cappelluti, F., and Gioannini, M., "Impact of carrier transport on the performance of qd lasers on silicon: a drift-diffusion approach," *Photonics Research* **8**(8), 1388–1397 (2020).

[13] Sears, K., Buda, M., Tan, H., and Jagadish, C., "Modeling and characterization of InAs/GaAs quantum dot lasers grown using metal organic chemical vapor deposition," *Journal of Applied Physics* **101**(1), 013112 (2007).

[14] Chen, S., Li, W., Wu, J., Jiang, Q., Tang, M., Shutts, S., Elliott, S. N., Sobiesierski, A., Seeds, A. J., Ross, I., et al., "Electrically pumped continuous-wave III–V quantum dot lasers on silicon," *Nature Photonics* **10**(5), 307 (2016).

[15] Duan, J., Huang, H., Dong, B., Norman, J. C., Zhang, Z., Bowers, J. E., and Grillot, F., "Dynamic and nonlinear properties of epitaxial quantum dot lasers on silicon for isolator-free integration," *Photonics Research* **7**(11), 1222–1228 (2019).

[16] Levine, A., Van Tartwijk, G., Lenstra, D., and Erneux, T., "Diode lasers with optical feedback: Stability of the maximum gain mode," *Physical Review A* **52**(5), R3436 (1995).

[17] Hohl, A. and Gavrielides, A., "Bifurcation cascade in a semiconductor laser subject to optical feedback," *Physical Review Letters* **82**(6), 1148 (1999).

[18] Heil, T., Fischer, I., Elsäßer, W., and Gavrielides, A., "Dynamics of semiconductor lasers subject to delayed optical feedback: The short cavity regime," *Physical Review Letters* **87**(24), 243901 (2001).

[19] Erneux, T., "Asymptotic methods applied to semiconductor laser models," in [*Physics and Simulation of Optoelectronic Devices VIII*], **3944**, 588–601, International Society for Optics and Photonics (2000).

[20] Ritter, A. and Haug, H., "Theory of laser diodes with weak optical feedback. I. small-signal analysis and side-mode spectra," *JOSA B* **10**(1), 130–144 (1993).